

# The Impact of Shared Autonomous Vehicles in Microtransit Systems: A Case Study in Atlanta

Jason Lu<sup>1,2</sup>, Tejas Santanam<sup>1</sup>, Hongzhao Guan<sup>\*1</sup>, Connor Riley<sup>1</sup>, Meen-Sung Kim<sup>1</sup>,  
Anthony Trasatti<sup>1</sup>, Neda Masoud<sup>2</sup>, and Pascal Van Hentenryck<sup>1</sup>

<sup>1</sup>H. Milton Stewart School of Industrial and Systems Engineering,  
Georgia Institute of Technology

<sup>2</sup>Department of Civil and Environmental Engineering,  
University of Michigan

December 10, 2025

## Abstract

Microtransit systems represent an enhancement to solve the first- and last-mile problem, integrating traditional rail and bus networks with on-demand shuttles into a flexible, integrated system. This type of demand responsive transport provides greater accessibility and higher quality levels of service compared to conventional fixed-route transit services. Advances in technology offer further opportunities to enhance microtransit performance. In particular, shared autonomous vehicles (SAVs) have the potential to transform the mobility landscape by enabling more sustainable operations, enhanced user convenience, and greater system reliability. This paper investigates the integration of SAVs in microtransit systems, advancing the technological capabilities of on-demand shuttles. A shuttle dispatching optimization model is enhanced to accommodate for driver behavior and SAV functionalities. A model predictive control approach is proposed that dynamically rebalances on-demand shuttles towards areas of higher demand without relying on vast historical data. Scenario-driven experiments are conducted using data from the MARTA Reach microtransit pilot. The results demonstrate that SAVs can elevate both service quality and user experience compared to traditional on-demand shuttles in microtransit systems.

**Keywords:** *Mobility, Public Transit, Microtransit, Shared Autonomous Vehicles, Model Predictive Control, Demand Responsive Transport*

---

\*Corresponding author: [hguan7@gatech.edu](mailto:hguan7@gatech.edu)

# 1 Introduction

The demand for mobility services has grown at an unprecedented rate with the proliferation of smartphone apps and the rise of the sharing economy [Chan and Shaheen, 2012, Standing et al., 2019]. These developments have fueled the rapid expansion of digital ridehailing systems such as Uber or Lyft, which provide convenient door-to-door transportation for mobility users [Wang and Yang, 2019]. However, traditional ridehailing services exhibit a few critical drawbacks. In particular, they contribute significantly towards empty miles, and by consequence exacerbate congestion in the road network and overall system efficiency [Erhardt et al., 2019, Henao and Marshall, 2019, Wu and MacKenzie, 2021, Beojone and Geroliminis, 2021]. By contrast, while traditional fixed-route transit services provide more sustainable mobility, their limited accessibility due to the first- and last-mile problem often hinders user adoption [Venter, 2020, Sogbe et al., 2024, Lu and Masoud, 2025a].

Microtransit, a demand responsive transport service, is an integrated mobility solution made up of on-demand services to enhance system efficiency and address the first- and last-mile problem for traditional bus and rail networks. Modern microtransit systems operated by transit agencies use human-operated on-demand vehicles, thereby limiting the potential efficiency of first- and last-mile services. In particular, transit agencies enforce safety protocols that prohibit drivers from using mobile devices when en-route between stops [Hart, 2009, Griffin et al., 2014]. From a user perspective, this can substantially prolong waiting times, as drivers cannot respond to new trip requests while driving even when a nearby passenger could be served with minimal deviation. From an operational standpoint, shuttles would incur unnecessary empty miles as shuttles may need to backtrack previously traveled routes to accommodate requests. Furthermore, when shuttles are idling, drivers could experience delayed responses to incoming requests due to inattention, further extending user waiting times. Shared autonomous vehicles (SAVs) present the opportunity to nullify these limitations, as their technologies enable dynamic rerouting of shuttles to promptly accommodate online user requests [Alonso-Mora et al., 2017, Bruglieri et al., 2024].

This paper studies the impact of SAVs in microtransit systems and evaluates their impact on system performance. It proposes the Unified Real-Time Dispatch and Control (URDC) framework, which consists of shuttle dispatching, routing, and rebalancing models. This framework features three key components. First, a Real-Time Dial-a-Ride System (RTDARS), which models shuttle routing and dispatching, is enhanced to capture driver behaviors. Second, the RTDARS-SAV is introduced to capture the operational capabilities of SAVs. Third, an optimization-based model predictive control (MPC) approach is developed that rebalances the shuttle fleet toward areas of higher demand without the need for extensive historical data. To evaluate the the impacts of SAV integration and other operational changes in the microtransit system, scenario-driven experiments were conducted based on MARTA Reach, a six-month microtransit pilot of an On-Demand Multimodal Transit System (ODMTS) prototype in the Metropolitan Atlanta area [Van Hentenryck et al., 2023]. The pilot was implemented in collaboration with the Metropolitan Atlanta Rapid Transit Authority (MARTA) and the Georgia Institute of Technology. ODMTS is an emerging type of microtransit system, where trains and buses operate on fixed schedules while shuttles operate dynamically to serve passengers' first- and last-mile connections. Passengers provide their desired origin and destination locations through a mobile application or via telephone, after which ODMTS provides a route to serve them.

The remainder of the paper is structured as follows. Section 2 reviews related work. Section 3 presents the methodology developed for this study. Section 4 describes the scenario-driven experiments based in the Atlanta metropolitan area and analyzes the results in terms of service quality and user benefits. Finally, Section 5 concludes with final remarks and future research.

## 2 Literature Review

Dial-a-Ride services have been highlighted by several studies, particularly in the context of dispatching and routing optimization. [Cordeau and Laporte \[2007\]](#) established several fundamental mixed-integer programming (MIP) formulations for the dial-a-ride problem (DARP). These formulations address two distinct cases: one in which trip requests are known a priori and another in which trip requests arise dynamically in real time. [Alonso-Mora et al. \[2017\]](#) were the first to address large-scale DARP, developing a heuristic that employs shareability graphs and cliques to generate feasible routes and a MIP model to select routes and perform matching of rider requests to vehicles. This approach was later enhanced by [Lowalekar et al. \[2018\]](#) through the use of zone paths. [Riley et al. \[2019\]](#) was the first algorithm to serve all requests in a large-scale setting, using column generation and an exponentially increasing penalty function for unserved requests. Hybrid methods have been proposed that combine routing recurrent requests offline while managing unexpected requests on-demand [[Tafreshian et al., 2021](#)].

As autonomous vehicle technology becomes more advanced and resilient, its integration in transit and mobility services becomes increasingly more feasible. [Litman \[2020\]](#) discussed the impact of SAVs on transport planning, highlighting their potential benefits, including reduced traffic and parking congestion, improved mobility, enhanced safety, energy savings, and emission reductions. More recent studies have shown that SAVs can induce a modal shift toward shared mobility, and that fleets of SAVs operating in conjunction with public transit systems can yield greater benefits than when operating independently [[Shaheen and Chan, 2016](#), [Salazar et al., 2018](#)]. [Levin et al. \[2019\]](#) and [Shen et al. \[2017\]](#) proposed methods for including SAVs as last-mile connectors for transit networks. [Lam et al. \[2016\]](#) designed a point-to-point public transit model serviced by SAVs. Simulation-based models have analyzed fleet sizing and operations for on-demand SAV fleets that serve first- and last-mile connections [Shen et al. \[2018\]](#), [Wang et al. \[2018\]](#). In hybrid simulation-optimization approaches, [Pinto et al. \[2020\]](#) designed a bi-level optimization framework where the upper level jointly determines transit route frequencies and SAV fleet sizes, and the lower level performs simulation for the traffic assignment of users. [Ng et al. \[2024\]](#) extended this study and designed a multicommodity network flow model that incorporates zonal clustering, cost-aware transit design, and route generation.

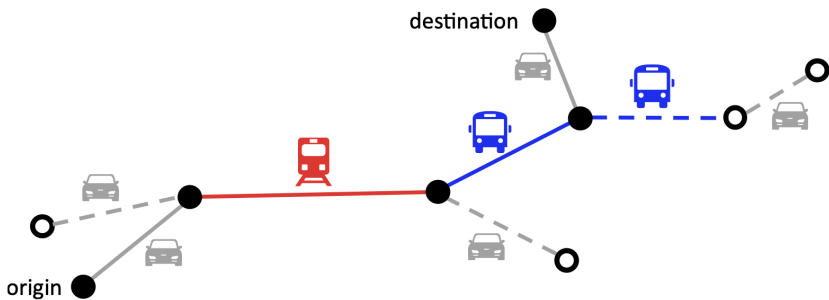


Figure 1: Example ODMTS with Passenger Path (solid lines)

MPC approaches have become increasingly important for repositioning in ridesharing and on-demand mobility systems, enabling improved routing efficiency, reduced waiting times, and lower operational costs. [Riley et al. \[2020\]](#) developed an MPC that employs vector autoregression to forecast weekly demand time series patterns to optimize taxi relocations across zones. [Wei et al. \[2023\]](#) proposed a reinforcement learning-based approach to generate reposition recommendations for vehicles combined with a linear programming (LP) formulation to model driver compliance behavior. MPC have become increasingly more relevant for au-

tonomous mobility-on-demand (AMoD) systems. [Zhang et al. \[2016\]](#) introduced two MIP MPC formulations for vehicle rebalancing, where vehicle rebalancing decisions are made according to the demand levels of the waiting customers. [Tsao et al. \[2018\]](#) extended this work to a stochastic MPC framework that incorporates predictions of short-term demand uncertainty. [Zgraggen et al. \[2019\]](#) modeled AMoD services as feeders to a transit system and designed an MPC for AMoD repositioning using demand forecasting and LP. More recently, [Aalipour and Khani \[2024\]](#) developed a finite-horizon control problem for MPC implementation in AMoD systems.

The case study presented in this paper is based on the MARTA Reach Pilot, which investigated the practical potential of ODMTS, an emerging type of microtransit system. The ODMTS system, initially proposed by [Maheo et al. \[2019\]](#), stems from the hub and shuttle transit system design introduced in earlier studies by [Campbell et al. \[2005\]](#). Figure 1 illustrates an example of an ODMTS and the path of a single passenger. In this example, a passenger is picked up by an on-demand shuttle for their first-mile leg near their origin and transported to a nearby train station. The passenger is then instructed to take a train followed by a bus, both of which operated on fixed schedules. When the passenger arrives at the bus station closest to the destination, another on-demand shuttle serves the last-mile leg for the passenger. This [video](#) from the [Socially Aware Mobility Lab \[2020\]](#) demonstrates this process. ODMTS provides significant advantages, including greater accessibility to transit systems, enhanced mobility for those without personal vehicles, and a cost-efficient business model [[Kodransky and Lewenstein, 2014](#), [Lazarus et al., 2018](#), [Stiglic et al., 2018](#), [McCoy et al., 2018](#)]. Case studies in Canberra, Australia [[Maheo et al., 2019](#)], Ann Arbor, Michigan [[Basciftci and Van Hentenryck, 2023](#)], and the metropolitan area of Atlanta, Georgia [[Auad et al., 2021](#), [Lu et al., 2024](#), [Guan et al., 2025](#)] demonstrate that ODMTS can simultaneously improve travel time, reduce system cost, and attract new passengers compared to existing transit systems. Furthermore, in addition to the aforementioned computational case studies, ODMTS has been piloted in Ann Arbor, Michigan [[Van Hentenryck, 2019](#)], Atlanta, Georgia [[Van Hentenryck et al., 2023](#)], and Savannah, Georgia [[Chatham Area Transit, 2025](#)], and has been technologically enhanced throughout the pilots.

Other case studies have also evaluated transit systems that incorporate on-demand services. [Bürklein et al. \[2021\]](#) simulated the effects of varying DRT fleet sizes and vehicle capacities for first-mile transit services in Markham, Canada. In another study, [Sanaullah et al. \[2021\]](#) evaluated an eight-month pilot in the city of Belleville, Canada, where late night fixed-route transit was supplemented with on-demand services.

## 2.1 Contributions

Despite a rich body of literature on DARP, MPC, SAVs and ODMTS, several clear gaps remain. Existing MPC approaches for repositioning typically rely on extensive historical data, which poses two key limitations: 1) insufficient data is available during service startup, and 2) the inability of models to easily accommodate short-term fluctuations in demand. Furthermore, prior studies on SAV integrations with transit systems do not provide comparisons between autonomous and non-autonomous services, particularly regarding key attributes such as dynamic vs non-dynamic re-routing and response times to requests when idling.

This study addresses these shortcomings by leveraging enhanced dispatching models, an MPC that does not require extensive historical data, and scenario-based experiments that focus on the impacts of varying levels of autonomy for shuttles. Thus, this paper is the first study that models SAVs to address microtransit challenges associated with human driving behaviors and the first study to conduct a case study using new and unique ODMTS pilot data. Specifically, the contributions of this paper are as follows:

1. This paper presents URDC: a comprehensive framework that leverages SAVs to overcome the operational limitations of human-driven shuttles in microtransit systems and to model shuttle repositioning without relying on extensive historical data.
2. To dispatch the shuttle fleet, this paper enhances the RTDARS dispatching model to incorporate human driver behavior modeling and introduces the RTDARS-SAV dispatching model to model the dynamic re-routing and immediate response times of SAV fleet operations. These two improvements lead to the design of scenario-driven experiments for microtransit systems, resulting in four distinct levels of fleet system competency and autonomy.
3. This paper conducts a case study in the Atlanta Metropolitan area using data from the MARTA Reach pilot, evaluating the effects of alternative fleet sizes, varying demand levels, and the integration of SAVs in microtransit systems. The results demonstrate the advantages of SAVs in microtransit systems in terms of both service quality and user convenience.

### 3 Unified Real-Time Dispatch and Control

The URDC framework consists of three central components: the RTDARS dispatching model, the RTDARS-SAV dispatching model, and the MPC.

The RTDARS dispatching model extends from [Riley et al. \[2019\]](#) and models real-time human-driven shuttle system dynamics, processing online trip requests while managing the routing of shuttles across the network. The RTDARS-SAV dispatching model extends from RTDARS and models SAV system dynamics, in particular, the zero-delay response times to requests and the on-demand dynamic re-routing of shuttles across the network. The MPC approach rebalances shuttles towards idle locations when not serving trip requests in both RTDARS and RTDARS-SAV. The notation used throughout the paper is summarized in Table 1.

#### 3.1 Preliminaries

Consider a finite time horizon  $\mathcal{T}$ , where each time step  $\tau \in [\mathcal{T}]$  corresponds to an epoch  $\epsilon_\tau$ . RTDARS processes requests by epochs, each of length  $l$ , and performs two tasks during each epoch: 1) batching the requests in the current epoch and 2) solving an optimization problem to assign and route unserved requests from previous epochs, minimizing the cost of service.

Table 1: Summary of notation.

Notation	Description
<i>Indices and sets</i>	
$T$	Finite set of time steps in the planning horizon.
$\tau$	Time index, $\tau \in [T]$ .
$\epsilon_\tau$	Epoch corresponding to time step $\tau$ .
$S$	Set of virtual stop locations (pickup and dropoff locations).
$S_{\text{idle}} \subseteq S$	Set of idle stops where shuttles are allowed to idle.

Continued on next page

Table 1: Summary of notation (continued).

Notation	Description
$R$	Set of all candidate shuttle routes.
$V$	Set of shuttles in the fleet.
$V_{\text{idle}} \subseteq V$	Set of idle shuttles with no current or future passengers.
$\hat{V}_{\text{idle}} \subseteq V_{\text{idle}}$	Set of idle shuttles that are not currently at an idle stop.
$N$	Set of unserved requests carried over from previous epochs.
$N_L \subseteq N$	Set of recent requests in the consideration window $L$ .
$D$	Set of potential driver response times.
<i>Request and route attributes</i>	
$p$	Pickup location of request $n$ , $p \in S$ .
$d$	Dropoff location of request $n$ , $d \in S$ .
$p_{\text{idle}}$	Closest idle stop to $p$ in terms of travel time, $p_{\text{idle}} \in S_{\text{idle}}$ .
$e$	Earliest possible pickup time of request $n$ .
$a_{rn}$	Parameter equal to 1 if request $n$ is served by route $r$ , and 0 otherwise.
$c_r$	Total waiting time accumulated from all requests served by route $r$ .
<i>Parameters</i>	
$l$	Length of an epoch, unit in seconds.
$L$	Length of the rolling consideration window for recent requests.
$Q_{\text{shuttle}}$	Passenger capacity of each shuttle.
$g_n$	Time dependent penalty for leaving request $n$ unserved in the current epoch.
$\delta$	Incentivization parameter that scales the growth of penalties $g_n$ .
$\gamma_s$	Number of recent requests mapped to idle stop $s$ (computed from $N_L$ ).
$\rho_s^v$	Travel time required to move shuttle $v$ to idle stop $s$ .
$t_{\epsilon_\tau}$	Start time of epoch $\epsilon_\tau$ .
$\hat{d}$	Sampled driver response time, $\hat{d} \sim \text{Unif}(D)$ .
$\Delta$	Driver response time threshold.
<i>Decision variables</i>	
$y_r$	Binary variable equal to 1 if route $r \in R$ is selected in the RTDARS master problem, and 0 otherwise.
$x_n$	Binary variable equal to 1 if request $n \in N$ remains unserved in the current epoch, and 0 otherwise.
$\zeta_s$	Integer variable for the number of shuttles to allocate to idle stop $s \in S_{\text{idle}}$ .
$z_s$	Auxiliary variable that acts as a proxy for $\zeta_s$ in the MPC objective.
$w_s^v$	Binary variable equal to 1 if shuttle $v \in \hat{V}_{\text{idle}}$ is relocated to idle stop $s \in S_{\text{idle}}$ , and 0 otherwise.
<i>Scenario descriptors</i>	
SFL I, SFL II, SFL III, SFL IV	Shuttle functionality levels representing different driver or SAV capabilities and idle stop policies.

Let  $S$  denote the set of virtual stop locations, which are potential user pickup and dropoff locations. Virtual stops are termed virtual as they do not require physical signage or infrastructure to mark their location, enabling more flexible placement within the service area. Shuttles are permitted to idle at idle stops, denoted by set  $S_{idle} \subseteq S$ . Unlike virtual stops, idle stops are carefully selected to account for geographical constraints and property restrictions, and therefore cannot be freely located.

Let  $R$  denote the set of all routes in the study area, comprising disjoint sets of requests. These routes are iteratively generated through an optimization-based routine, the details of which can be found in [Riley et al. \[2019\]](#). Let  $c_r$  represent the total waiting time accumulated from all requests served by route  $r \in R$ . The set  $V$  denotes the set of shuttles, where each shuttle  $v \in V$  could serve a subset of routes  $R_v \subseteq R$ . The number of passengers per shuttle is limited by the shuttle capacity  $Q_{shuttle}$ , which is constant across all shuttles. An idle shuttle, which does not have any current nor future planned passengers, is denoted as  $v \in V_{idle}$ . Additionally,  $\hat{V}_{idle}$  denotes the set of idle shuttles that are not currently at an idle stop.

Let  $N$  represent the set of requests that remain unserved from previous epochs. Each request is represented by a tuple  $n = (p, d, p^{idle}, e) \in N$ , where  $p \in S$  is the pickup location,  $d \in S$  is the drop-off location,  $p^{idle} \in S_{idle}$  is the closest idle stop to  $p$  in terms of travel time, and  $e$  is the earliest possible pickup time. The auxiliary parameter  $a_n^r$  is set to 1 if request  $n$  is served by route  $r$  and 0 otherwise. For recent trips, the set  $N_L$  denotes the collection of trip requests occurring within the consideration window  $L$ , which is updated at each epoch.

An unserved request  $n \in N$  incurs a time-dependent penalty  $g_n = \delta 2^{(2\tau - e)/10l}$ , which increases with each additional epoch until the request has been served. This prioritizes requests that have experienced longer waiting times. Here,  $\delta$  is an incentivization parameter that weights scheduling in the earliest available epoch. At the end of each epoch, new requests are introduced into the system and penalties for unserved requests from previous epochs are updated. RTDARS guarantees that all requests are ultimately served, leaving no passengers unserved after all epochs have been processed.

$$\text{minimize} \quad \sum_{r \in R} c_r y_r + \sum_{n \in N} g_n x_n, \quad (1a)$$

$$\text{subject to} \quad \sum_{r \in R} y_r a_n^r + x_n = 1 \quad \forall n \in N, \quad (1b)$$

$$\sum_{r \in R_v} y_r = 1 \quad \forall v \in V, \quad (1c)$$

$$x_n \in \{0, 1\} \quad \forall n \in N, \quad (1d)$$

$$y_r \in \{0, 1\} \quad \forall r \in R \quad (1e)$$

### 3.2 RTDARS

The epoch-based optimization considers both the waiting times incurred when serving requests and penalties associated with unserved requests in previous epochs. Shuttles already committed to serving routes from earlier epochs remain unavailable until their current services are completed. To maintain service quality, routes for shuttles are constrained to ensure that passengers do not significantly deviate from their ideal paths.

This study employs the column generation algorithm for RTDARS from [Riley et al. \[2019\]](#) to solve the epoch-based optimization problem. The algorithm iteratively selects shuttle routes through a master

problem and generates new shuttle routes through a pricing subproblem, representing new columns in the master problem. After meeting a stopping criteria, the column generation algorithm selects the optimal combination of routes. Model 1 presents the master problem formulation for RTDARS column generation algorithm. The binary decision variables  $y_r = 1$  if route  $r \in R$  is used in the solution and  $x_n = 1$  if request  $n$  remains unserved by any route in the solution. Objective (1a) minimizes the total waiting times across selected routes and penalty costs from unserved requests. Constraint (1b) ensures that requests are either served by a shuttle or left unserved. Constraint (1c) ensures that shuttles are assigned to a single route. Constraints (1d) and (1e) define the binary conditions for decision variables  $x_n$  and  $y_r$ , respectively.

### 3.2.1 Modeling Driver Behavior in RTDARS

In practice, idling drivers exhibit inconsistent response times to trip assignments and rebalancing instructions. Consider a full set of potential driver response times  $D = \{d_1, \dots, d_{|D|}\}$ , where each response time is assumed to have an equal probability of occurrence. During the execution of RTDARS, if a shuttle is unoccupied during any epoch, the driver will act on the next instruction received with a uniformly sampled response time such that the observed response time  $\hat{d} \sim \text{Unif}(D)$ . Note that identical response times may appear within  $D$ , implying a higher probability of selecting response times that occur more frequently in the set. Although drivers may not respond at all in practice, requiring requests to be reallocated, we assume that all drivers respond within a threshold  $\Delta$  such that any observed response time satisfies  $\hat{d} \leq \Delta$ .

## 3.3 Model Predictive Control

Riley et al. [2019] assumed that shuttles could idle freely at any location until the next request arrived. However, this assumption is no longer practical for microtransit operations due to traffic, safety, and land ownership impediments. This study introduces a procedure to rebalance inactive shuttles to designated idle stops that have potential for higher user demand in the nearby area. Previously, Riley et al. [2020] proposed a learning-based approach to direct shuttles to high-demand regions. However, this requires substantial historical ridership data, which may not be available in many deployment contexts at the early stages. In contrast, this procedure models relocation policies that do not depend on extensive data availability.

The objective is to rebalance idle shuttles toward areas of high demand while ensuring that shuttles only idle at stops within  $S_{idle}$ . Equation (2) computes the number of recent requests  $N_L$  mapped to each idle stop, where  $\mathbb{I}$  is a binary indicator function.

$$\gamma_s = \sum_{n \in N_L} \mathbb{I}[p^{idle} = s] \quad \forall s \in S_{idle} \quad (2)$$

Model (3) rebalances the shuttle fleet, determining the desired number of shuttles, defined as the decision variable  $\zeta_s$ , to allocate at each idle stop  $s \in S_{idle}$ , given the values of  $\gamma_s$ . Objective (3a) minimizes the total ratio of requests,  $\gamma_s$ , to shuttles,  $z_s$ , a proxy for  $\zeta_s$ , across all idle stops. Constraint (3b) preserves the validity of the objective function by preventing division errors via  $z_s$  when  $\zeta_s = 0$  and implicitly doubles the penalty associated with assigning zero shuttles to an idle stop compared to assigning one. Constraint (3c) ensures that the total number of shuttles assigned across all idle stops equals the total number of idle shuttles available. The model considers only the set  $\hat{V}_{idle}$  rather than the  $V_{idle}$  to avoid relocating shuttles already at an idle stop, which incurs higher cost of resources. Constraint (3d) defines  $\zeta_s$  as a non-negative integer decision variable.

$$\text{minimize} \quad \sum_{s \in S_{idle}} \frac{\gamma_s}{z_s}, \quad (3a)$$

$$\text{subject to} \quad z_s = \max\{0.5, \zeta_s\} \quad \forall s \in S_{idle}, \quad (3b)$$

$$\sum_{s \in S_{idle}} \zeta_s = |\hat{V}_{idle}| \quad , \quad (3c)$$

$$\zeta_s \in \mathbb{N}^0 \quad \forall s \in S_{idle} \quad (3d)$$

Model (3) returns the number of shuttles  $\zeta_s$  desired at idle stop  $s \in S_{idle}$ . However, it does not identify which specific shuttles should be relocated. To address this, Model (4) presents a MIP for shuttle relocation, which takes the desired shuttle allocation count  $\zeta_s$  from Model (3) as input. The binary decision variable  $w_s^v = 1$  if shuttle  $v \in \hat{V}_{idle}$  is chosen to relocate to stop  $s \in S_{idle}$ . Objective (4a) minimizes the total travel time  $\rho_s^v$  to move each shuttle  $v \in \hat{V}_{idle}$  to each idle stop  $s \in S_{idle}$ . Constraint (4b) ensures the correct number of shuttles are assigned to each idle stop. Constraint (4c) ensures that all shuttles relocate to exactly one idle stop. Lastly, constraint (4d) defines binary conditions for  $w_s^v$ .

It is important to note that Model (3) could induce tied solutions under Objective (3a), which can influence the solution of Model (4). Appendix A extends the model to incorporate tie-breaking procedures that resolve such cases.

$$\text{minimize} \quad \sum_{v \in \hat{V}_{idle}} \sum_{s \in S_{idle}} \rho_s^v w_s^v, \quad (4a)$$

$$\text{subject to} \quad \sum_{v \in \hat{V}_{idle}} w_s^v = \zeta_s \quad \forall s \in S_{idle}, \quad (4b)$$

$$\sum_{s \in S_{idle}} w_s^v = 1 \quad \forall v \in \hat{V}_{idle}, \quad (4c)$$

$$w_s^v \in \{0, 1\} \quad \forall s \in S_{idle}, v \in \hat{V}_{idle} \quad (4d)$$

### 3.4 RTDARS-SAV

Consistent with standard driver distraction policies adopted by transit agencies, the RTDARS dispatching model from Riley et al. [2019] prohibits re-routing shuttles once they are en route to their next stop. SAVs are not subject to such restrictions, as they can dynamically re-route in response to on-demand requests. This study designs a modified RTDARS enhanced with SAV routing: RTDARS-SAVs.

In RTDARS, when driver-operated shuttles becomes idle, they are dispatched to a predetermined idle location and cannot deviate from this plan, even if a new requests arise while deadheading. The optimization routine treats this procedure on an epoch basis. When optimizing for epoch  $\epsilon_\tau$  with start time  $t_{\epsilon_\tau}$ , an estimate of the system state at  $t_{\epsilon_{\tau+1}}$  is passed to the optimization routine. For RTDARS-SAVs, routing decisions are determined using the shuttle's predicted location at  $t_{\epsilon_{\tau+1}}$ . Consequently, within the simulation, SAVs can be re-routed dynamically between stops, allowing for greater flexibility and responsiveness in real-time operations.

Furthermore, there is no need to model driver behavior as SAVs exhibit zero delay responses to requests when idling. In RTDARS-SAV, the driver behavior modeling component discussed in Section 3.2.1 is

eliminated.

## 4 Case Study

This study uses data from the MARTA Reach Pilot in Atlanta by [Van Hentenryck et al. \[2023\]](#). The MARTA Reach pilot integrated on-demand shuttles to serve users with MARTA’s fixed-route bus and rail services, representing a pivotal development towards ODMTS in practice. This integration operated in conjunction with the broader transit network and in close cooperation with the MARTA.

### 4.1 Pilot Operations

The MARTA Reach pilot operated for six months, from March 1st to August 31st, 2022. Daily operations went from 6 A.M. to 7 P.M. on weekdays, including federal holidays, for a total of 132 service days. Passengers within the pilot zones provided could request trips by providing their origins and destinations through a mobile application or via telephone. Operations were divided into two phases. Phase 1 lasted from the pilot’s introduction on March 1st, 2022 to May 15, 2022, where MARTA Reach operated in three distinct zones: Belvedere, West Atlanta, and Gillem. Phase 2 lasted from May 16, 2022 to the pilot’s end on August 31, 2022. During this phase, the three initial zones all expanded, and North Fulton was included as an additional zone. All requests were geo-fenced such that trip pickup and dropoffs only occurred within the same zone. Trips can either connect users to a transit station or serve as direct trips, where users travel directly from their pickup to drop-off locations. Users are charged a fixed fare regardless of trip type. In particular, passengers connecting to a fixed-route service pay the same fare and are not required to pay an additional fee for the transfer. Full details of the MARTA Reach pilot are available in [Van Hentenryck et al. \[2023\]](#).

This study focuses on 2 of the 4 MARTA Reach zones: West Atlanta and Belvedere. These two zones accounted for the majority of ridership, with 58.45% and 34.81% of all requests being served from West Atlanta and Belvedere, respectively. Furthermore, both zones included portions of the MARTA rail network, enabling the integration of on-demand shuttle services with fixed-route transit and supporting multimodal connectivity. In Phase 2, the West Atlanta zone operated with six shuttles during the pilot and the Belvedere zone operated with four.

For experimental analysis, this study uses MARTA Reach ridership data from August 31, 2022, the day with the highest ridership observed during the pilot.

Shuttle operations were conducted with eight-passenger vehicles across two daily driver shifts: 6 A.M. to 1 P.M. and 1 P.M. to 7 P.M. When receiving a trip request, the pilot system’s optimization routine determined vehicle assignments. Safety protocols of MARTA dictated that drivers were not permitted to handle on-demand received requests or make routing changes while en route between stops. Shuttle pickup and dropoff operations were restricted to virtual stops, designated via geosensing technology implemented during the pilot. Virtual stops were pre-approved by MARTA for both pedestrian and driver safety. Unlike conventional bus stops, virtual stops did not necessarily have physical signage. Virtual stops were positioned to sufficiently cover the MARTA Reach zones, providing convenient passenger access while maintaining operational efficiency and safety.

Figure [2a](#) and [2b](#) display the virtual stops and idle locations for the Belvedere and West Atlanta zones, respectively. The blue markers represent MARTA fixed-route stops and were essential for multimodal connections to bus and rail lines. The orange markers represent additional stops introduced during MARTA

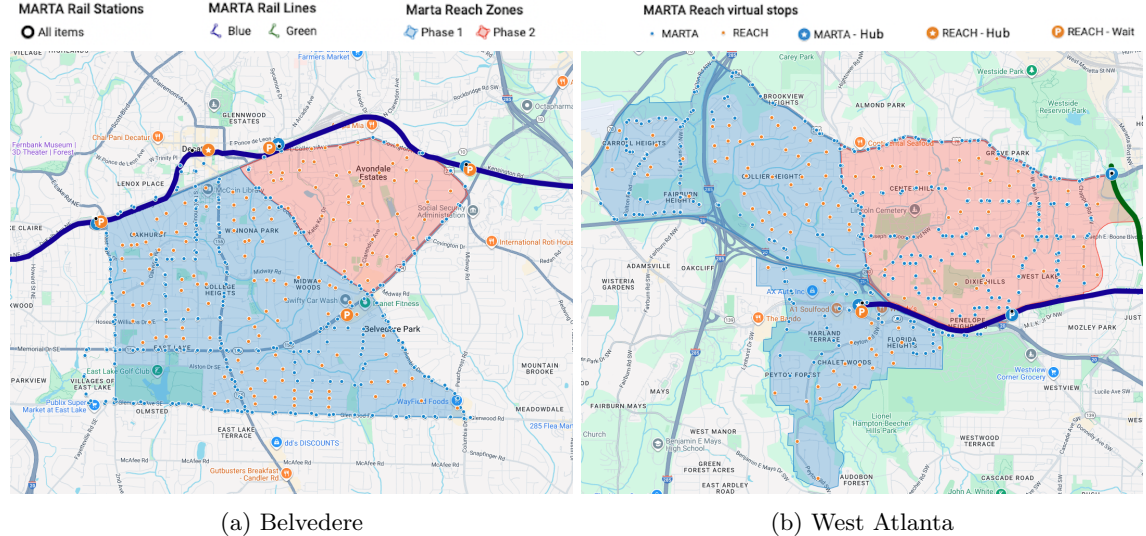


Figure 2: Belvedere and West Atlanta MARTA Reach zones (blue zones correspond to phase 1 deployment areas and pink zones correspond to phase 2 expansions of deployment areas)

Zone	Total ( $ S $ )	Existing MARTA stops/stations	New MARTA Reach stops	Idle stops ( $ S_{idle} $ )	# Shuttles ( $ V $ )
Belvedere	465	308	157	4	4
West Atlanta	485	374	111	3	6

Table 2: Zone Details of Pilot on August 31, 2022

Reach to serve passengers. When not serving passengers, shuttles were restricted to idling in designated idle locations selected by MARTA, which prevents unnecessary congestion, safety hazards, and land ownership conflicts. Drivers were required to proceed to one of the approved idle locations in their zone when not assigned to any active requests. Table 2 summarizes the makeup of virtual and idle stops, as well as the number of operational shuttles, in Belvedere and West Atlanta.

## 4.2 Experimental Scenarios

The experimental scenarios in this study are defined by three attributes: fleet size, fleet functionality, and ridership level. The distinct combinations of all these attributes constitute the total set of experimental scenarios simulated for each zone. Table 3 summarizes the scenario attributes for Belvedere and West Atlanta.

Zone	Belvedere	West Atlanta
Fleet Sizes ( $ V $ )	3,4,5	5,6,7
SFLs	<i>I, II, III, IV</i>	
Ridership Levels ( $ N $ )	Base (1x), 2x, 3x	

Table 3: Summary of Scenario Makeups

#### 4.2.1 Fleets

Three fleet sizes are examined for each zone. The baseline fleet size corresponds to that used during the MARTA Reach Pilot: four shuttles in Belvedere and six shuttles in West Atlanta. The other two fleet size configurations for each zone are created by incrementing or decrementing the baseline fleet size by one vehicle.

#### 4.2.2 Shuttle Functionality Levels

The shuttle fleets are classified into four shuttle functionality levels (SFLs), reflecting the degree of automation and routing capability, summarized below:

- **SFL *I*** - Level 1 functionality: Human-driven shuttles with variable response times to passenger requests while idling at stops. This serves as the base SFL for modern microtransit pilot systems.
- **SFL *II*** - Level 2 functionality: Human-driven shuttles with zero-delay response times when idling at stops
- **SFL *III*** - Level 3 functionality: SAVs with zero-delay response times and dynamic re-routing capabilities to accommodate on-demand requests. While SAVs do not require any labor breaks, they do require maintenance such as recharging and thus continue to operate in shifts.
- **SFL *IV*** - Level 4 functionality: SFL *III* but with idle stops relocated to the most frequent origin points of trip requests at the start of each shift.

Table 4 provides a concise summary of the attributes of each SFL and the dispatching models used to solve them. SFL *I* represents operational attributes of the MARTA Reach pilot, while SFL *III* reflects those of SAV operations. SFLs *II* and *IV* serve as idealized operational performance scenarios corresponding to SFLs *I* and *III*, respectively.

SFLS	Dispatching Model	Driver	Delay	Idle Locations
<i>I</i>	RTDARS	Human	Uniform	Predetermined and fixed
<i>II</i>	RTDARS	Human	0	Predetermined and fixed
<i>III</i>	RTDARS-SAV	SAV	0	Predetermined and fixed
<i>IV</i>	RTDARS-SAV	SAV	0	Unrestricted and flexible

Table 4: Summary of SFL Attributes

The idle relocation procedure for SFL *IV* occurs twice daily and assumes full knowledge of all requests throughout the day. At the start of each shift, idle stops are repositioned based on the most common trip origins observed during the respective shift. The number of idle stops remains constant across all experiments and only locations are updated.

#### 4.2.3 Ridership Sampling

To evaluate the impact of higher ridership levels on system performance, this study scales ridership by sampling trip requests from the days preceding August 31, 2022, the base experimental day, until a desired ridership level is achieved. This allows consideration of double and triple the baseline trip volumes for both Belvedere and West Atlanta zones. Only requests within Phase 2 of MARTA Reach are included as the base

experimental day occurred during Phase 2 operations. Trips from a user already sampled were included only if its time window does not overlap with any existing time window of the user. This ensures that synthetic ridership increases reflect realistic temporal distributions without duplicating passenger activity.

#### 4.2.4 Pilot Driver Behavior Sampling

During the MARTA Reach pilot, observed driver response delays for trip requests introduced challenges that adversely affected operations. As such, an analysis of driver response times to passenger trip requests was conducted, and the resulting response time distribution was incorporated into the experimental design.

To ensure reliability, the analysis focused on the month of August, which exhibited the highest ridership, stable service operations, and full deployment of all MARTA Reach functionalities [Van Hentenryck et al., 2023]. 1619 trips were analyzed in which shuttles were idle and subsequently dispatched to a passenger’s requested origin stop. This subset was selected because delays in such cases could be more reasonably attributed to driver behavior, whereas delays during active service were typically operational in nature and not indicative of driver inattention.

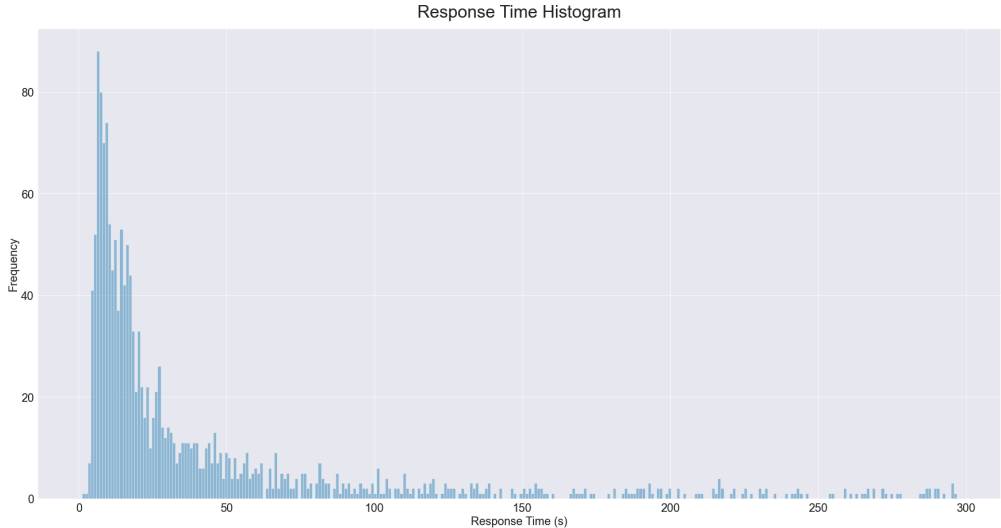


Figure 3: Driver Response Time Distribution

Figure 3 illustrates the distribution of driver response times, which is right-skewed with a mean response time of 43.14 seconds and a median response time of 18 seconds. The distribution indicates that half of the drivers responded promptly, on average within a minute. However, the extended right tail reveals occasional prolonged response times, suggesting intermittent issues related to driver attentiveness or delayed responsiveness.

### 4.3 Experimental Setup

With all combinations of fleet sizes, modes, and ridership levels, a total of 36 experimental scenarios were simulated for each zone, with 72 total scenarios.

The time and distance between virtual stops was estimated using real data obtained during the pilot period and data from OpenStreetMap using the Graphhopper API [OpenStreetMap contributors, 2017]. Baseline values were initially obtained from OpenStreetMap, which provided the shortest possible time and

Parameter	Value
Lower Bound Time	6 (MARTA Reach operations begin at 6 A.M.)
Upper Bound Time	19 (MARTA Reach operations end at 7 P.M.)
$Q^{shuttle}$	6 (minivan DRT microtransit services)
$l$	30 seconds ([ <a href="#">Riley et al., 2019</a> ])
$\delta$	420 seconds ([ <a href="#">Riley et al., 2019</a> ])
$L$	1 hour (MARTA Reach)
$\Delta$	300 seconds (MARTA Reach)

Table 5: Relevant Experimental Parameters

distance values. These values were subsequently scaled to reflect congested traffic using travel time collected from the pilot zones. Outliers resulting from glitches or systematic errors in the data were excluded, and a simple linear regression was fitted using the remaining data.

For all scenarios, shuttles were initially distributed uniformly across idle stops within each zone. For SFL  $I$ , driver response times  $D$  were sampled from the response times of MARTA Reach drivers discussed in Sections 3.2.1 and 4.2.4.

The base level of ridership for the Belvedere zone considers 39 completed trips (43 users) for the base day of August 31, 2022. With sampling from preceding pilot days, 2x ridership considers 78 completed trips (82 users), and 3x ridership considers 117 completed trips (122 users). West Atlanta considers 82 completed trips (89 users) from the base day, 164 completed trips (181 users) for 2x ridership, and 246 completed trips (267 users) for 3x ridership. Each trip could have multiple users, accommodating up to four for a single trip request.

Table 5 summarizes the key framework parameters. The lower and upper bound times match the duration for a single day of MARTA Reach. Shuttle capacity was set to 6, consistent with a typical minivan. Minivans were chosen over sedans to account for the larger vehicle capacities often required in public transit operations. Although sedans may be more cost-efficient, transit agencies are non-profit, where service quality and accessibility are prioritized. Furthermore, this configuration supports possible integration with paratransit services. First, paratransit fleets typically accommodate six or more passengers, allowing these services to leverage existing vehicles rather than investing in new shuttles. Second, ODMTS was piloted alongside paratransit services, and in the future paratransit services can transition into on-demand operations using a reservation-based system [[Chatham Area Transit, 2025](#)].  $l$  and  $\delta$  were set to 30 seconds and 420 seconds, respectively, consistent with the effective parameter values identified by [Riley et al. \[2019\]](#) when balancing computational efficiency and request frequency. The trip consideration window  $L$  was set to one hour and the response time threshold  $\Delta$  was set to 300 seconds, identical to the MARTA Reach pilot. RTDARS and RTDARS-SAV were implemented in C++ and used Gurobi 9.5.0 to solve MIPs.

#### 4.4 Analysis of Waiting and Travel Times

Figures 4a and 4b present the average waiting time per request across different SFLs and fleet sizes at the base ridership level for Belvedere and West Atlanta, respectively. Dots indicate mean values and bars represent one standard deviation from the mean. Evidently, under the same ridership scenario, increasing the fleet size consistently reduces waiting times in both zones, as more shuttles can accommodate demand simultaneously.

In the context of SFLs, SFLs  $I$  and  $II$ , which involve human drivers, the average wait times range

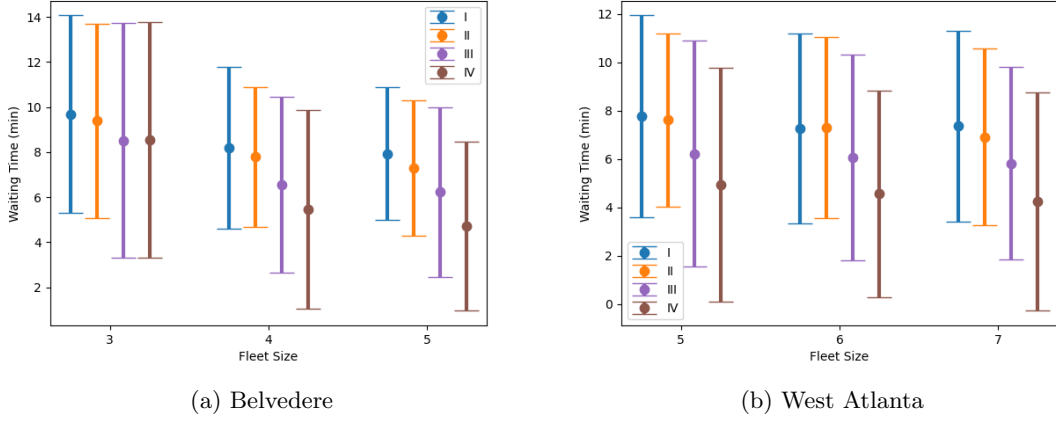


Figure 4: Average Waiting Time Per Trip Across SFLs at Base Ridership Level

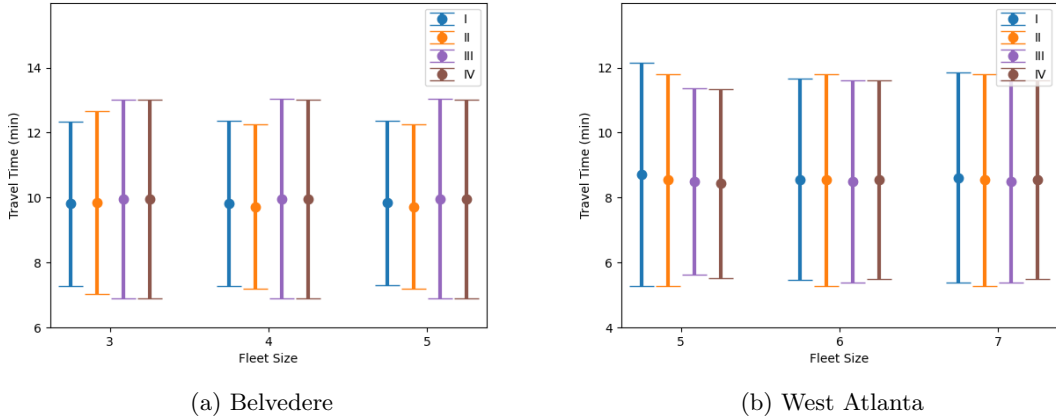


Figure 5: Average Travel Time Per Trip Across SFLs at Base Ridership Level

between 7-10 minutes for Belvedere and 6-8 minutes for West Atlanta. As expected, eliminating driver response delays in SFL *II* yields slightly lower waiting times than SFL *I*. While the average improvement is modest, eliminating driver responses prevents instances of excessively long waiting times that can occur with human drivers, as previously illustrated in Figure 3. In both zones, the introduction SAVs substantially reduces passenger waiting times. Average waiting times decrease notably from SFL *II* to *III*, representing the transition from human-driven shuttles to SAVs. The waiting time reduction, up to two minutes under base ridership demand, is accompanied by narrower standard deviation ranges, indicating more consistent service and that most riders experience shorter waiting times. The benefits are further amplified in SFL *IV*, which relocates idle stops toward frequent origin points. This indicates that combining SAVs with demand-responsive idle stops offers the greatest improvement in service quality and operational efficiency. Even though all trips are guaranteed service, the vast majority of trips experience reasonable waiting times. Across all SFLs and fleet sizes, the 95th percentile waiting times are 19.35 minutes in Belvedere and 14.89 minutes in West Atlanta, demonstrating that users can be served conveniently under the base ridership scenario.

While SAVs may introduce additional detours to accommodate on-demand requests and reduce passenger

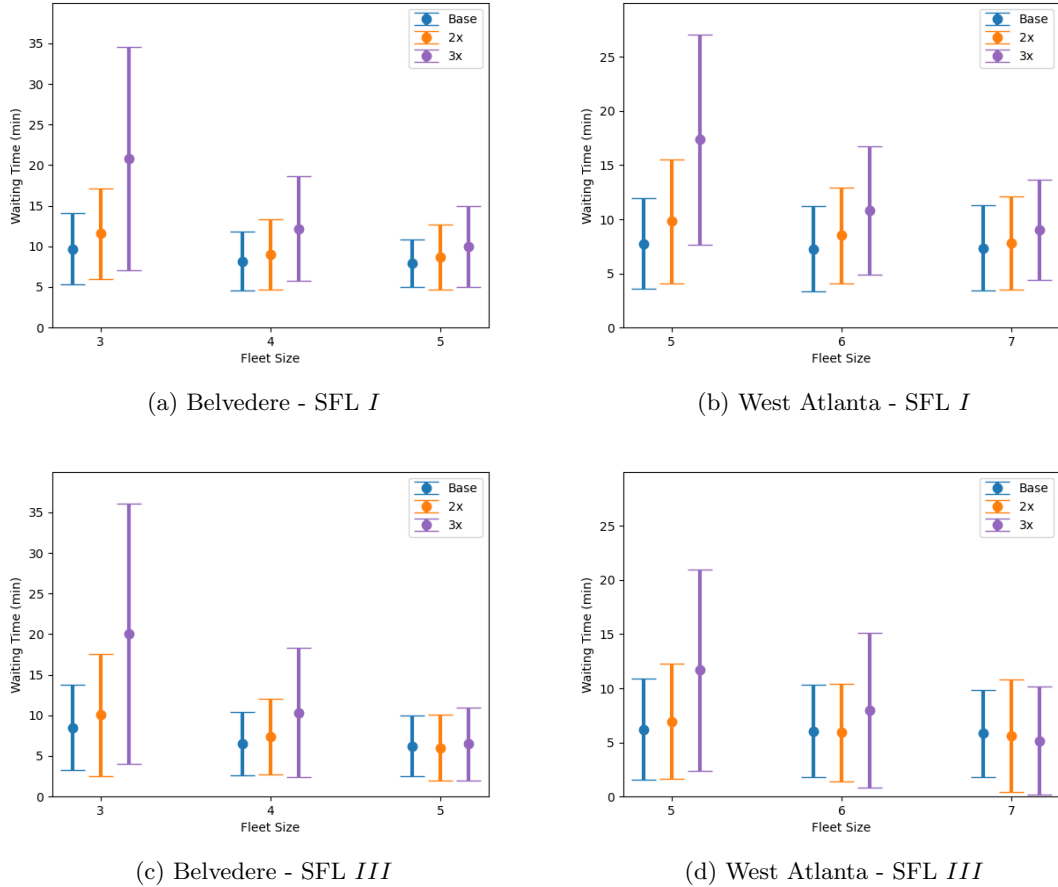


Figure 6: Average Waiting Time Per Trip Across Ridership Levels

waiting times, these detours do not compromise overall travel times for trips. Figures 5a and 5b show the average travel time per request across different SFLs and fleet sizes at the base ridership level for the Belvedere and West Atlanta zones, respectively. The results indicate that travel times remain largely unchanged between SFLs *II* and *III*, suggesting that any additional detours from more dynamic pickups introduced by SAV operations do not negatively impact trip durations. This outcome demonstrates that the RTDARS-SAV dispatching model effectively routes shuttles to balance detour flexibility with service efficiency, thereby maintaining high service quality.

Figure 6 illustrates the effects of higher ridership on the average wait times for SFLs *I* and *III*, respectively, in both Belvedere and West Atlanta. Across both SFLs, the trends are consistent: at lower fleet sizes, 3x ridership leads to pronounced increases in waiting times, reflecting an over-saturated system. Large standard deviations suggest that some riders are severely impacted. However, expanding the fleet size alleviates these effects by improving the system's capacity to serve additional passengers. Across all SFLs and fleet sizes at 3x ridership, the 95th percentile waiting times reach 53.05 minutes in Belvedere and 37.13 minutes in West Atlanta, which are considerably high. However, given the elevated demand levels, these longer waiting times could be substantially reduced by increasing the fleet size, as additional vehicles would improve service capacity under higher ridership conditions.

## 4.5 Analysis of Shuttle Distances

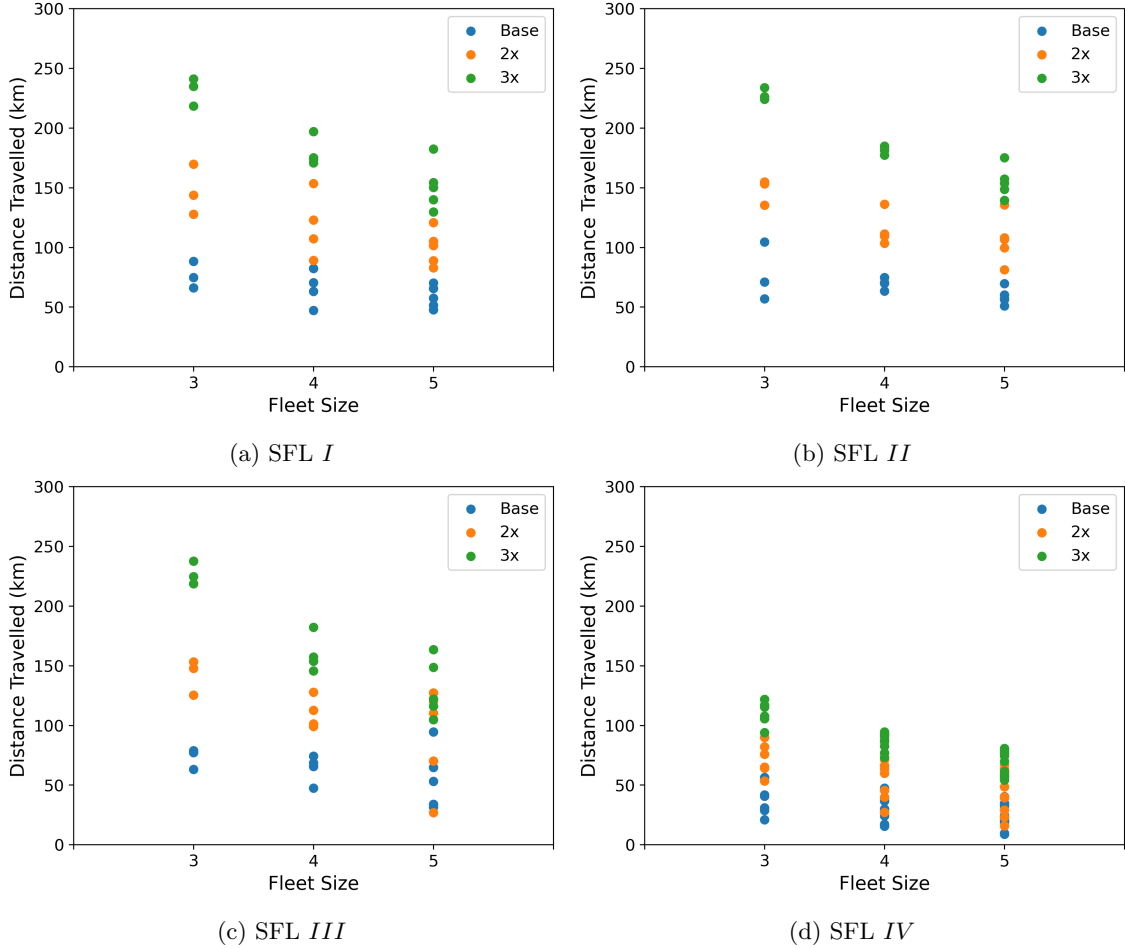


Figure 7: Distance Traveled by Each Shuttle in Belvedere

Figures 7 and 8 present the total kilometers traveled by each shuttle in Belvedere and West Atlanta, respectively, across different SFLs. Each point represents an individual shuttle under a particular combination of fleet size, ridership, and SFL. As expected in both zones, increasing the fleet size generally reduces the distance traveled by shuttles, as a larger number of vehicles share the same overall ridership. Conversely, the total distance traveled increases as ridership levels increase, reflecting the need to cover greater distances to accommodate more trip requests.

The sustainability benefits of SAVs are evident from the travel distance insights. Shuttles of SFL *III* travel fewer kilometers on average compared to shuttles of SFLs *I* and *II*, primarily due to their ability to dynamically re-route and serve requests en route. For SFLs *I* and *II*, shuttles with human drivers may need to backtrack routes to accommodate requests they could not serve while driving, resulting in greater kilometers traveled. Notably, SFL *IV* scenarios yield the shortest distance traveled. Since SFL *IV* incorporates strategic idling at locations with higher anticipated demand, shuttles are positioned closer to future requests, minimizing travel distances. This underscores the sustainability advantages of SFL *IV* and the value of strategically planning idle location placement in response to spatial and temporal demand patterns.

The shuttle distances also validate the effectiveness of both RTDARS and RTDARS-SAV dispatching models in effectively dispatching and managing shuttle fleets across all scenarios. Under any scenario, all shuttles exhibit relatively similar travel distances, indicating balanced utilization of shuttle fleets.

It is noteworthy that throughout all scenarios, shuttles traveled no more than approximately 300 kilometers throughout the entire simulation day. Assuming that SAVs are electric and begin the day with a full charge, this distance remains well within the typical range of modern electric minivans, which can exceed 350 kilometers on a single charge [Mercedes, 2025, Volkswagen, 2025].

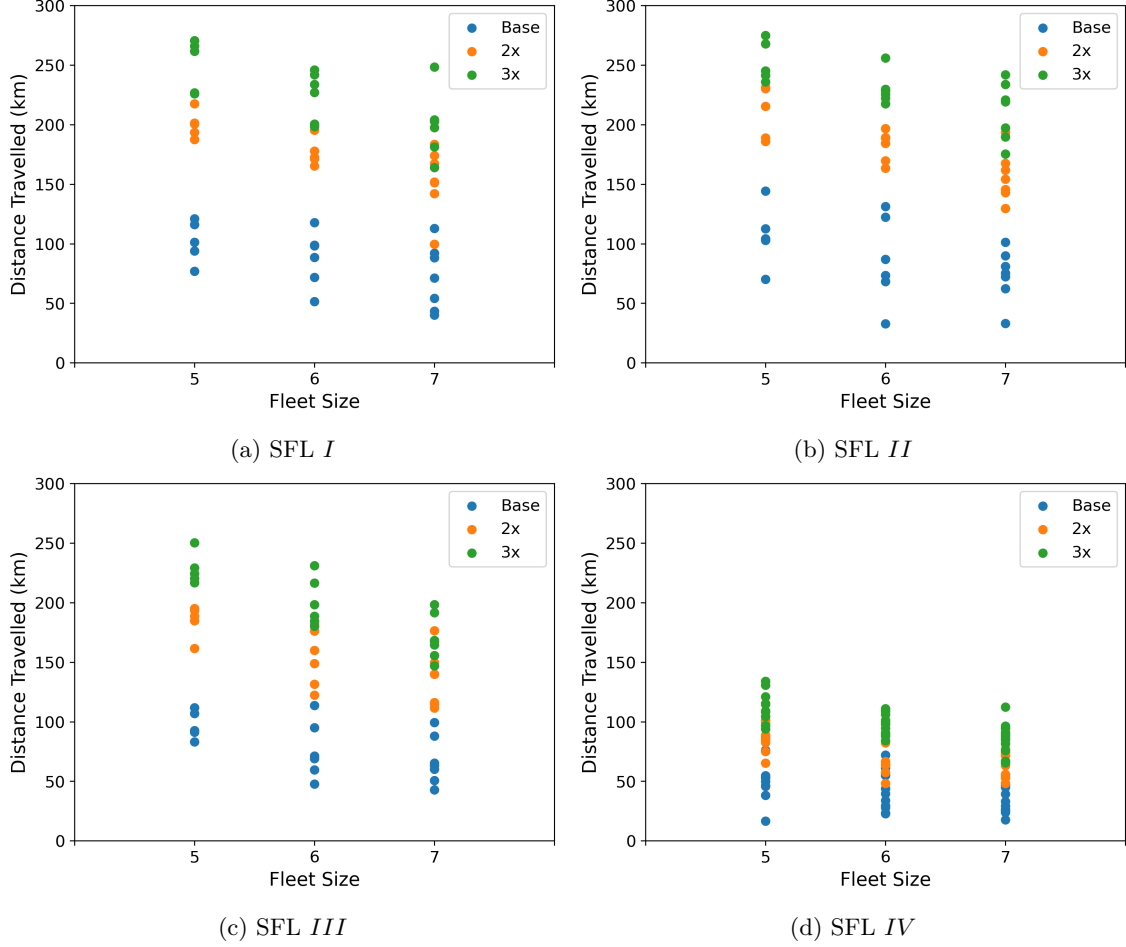


Figure 8: Distance Traveled by Each Shuttle in West Atlanta

Tables 6 and 7 show the empty kilometers for the shuttle fleets. The analysis indicates that SAVs have substantial potential to reduce not only travel kilometers traveled, but also total empty kilometers traveled by the fleet, especially as the fleet size increases. In Belvedere, SFLs *III* and *IV* consistently result in lower total kilometers traveled across all fleet sizes and ridership levels compared to SFLs *I* and *II*. Moreover, the kilometer savings generally grow at an increasing rate with both fleet size and ridership level. A similar pattern is observed in West Atlanta, where SFLs *III* and *IV* demonstrate consistent reductions in empty kilometers over SFLs *I* and *II*.

Even as ridership increases, fleets operating under SFLs *III* and *IV* maintain shorter empty kilometers than SFLs *I* and *II*. While total empty kilometer increases for all SFLs with increasing ridership, the

SFL	$ N  = 39$ : 1x (Base)			$ N  = 78$ : 2x			$ N  = 117$ : 3x		
	$ V  = 3$	$ V  = 4$	$ V  = 5$	$ V  = 3$	$ V  = 4$	$ V  = 5$	$ V  = 3$	$ V  = 4$	$ V  = 5$
<i>I</i>	98.4	132.2	161.8	200.1	226.8	257.4	304.5	334.2	366.1
<i>II</i>	104.1	147.6	163.5	207.4	222.0	292.3	310.5	339.2	387.6
<i>III</i>	88.6	124.9	147.1	182.5	201.9	213.4	299.1	252.5	264.5
<i>IV</i>	88.6	105.5	109.6	186.5	192.6	194.7	285.8	296.5	304.8

Table 6: Total Empty Kilometers for Fleets in Belvedere,  $|N|$  is the number of trip requests and  $|V|$  is the fleet size

SFL	$ N  = 82$ : 1x (Base)			$ N  = 164$ : 2x			$ N  = 246$ : 3x		
	$ V  = 5$	$ V  = 6$	$ V  = 7$	$ V  = 5$	$ V  = 6$	$ V  = 7$	$ V  = 5$	$ V  = 6$	$ V  = 7$
<i>I</i>	276.2	285.3	264.8	490.5	569.7	560.6	552.1	629.0	685.8
<i>II</i>	293.2	273.8	273.9	548.8	589.6	587.6	564.8	660.2	752.8
<i>III</i>	236.9	211.1	224.6	420.3	415.6	440.6	446.9	486.0	478.2
<i>IV</i>	272.0	271.7	281.0	405.4	393.5	442.5	435.7	466.3	471.8

Table 7: Total Empty Kilometers for Fleets in West Atlanta

consistency of SAVs in reducing kilometers driven signifies a notable operational benefit. In particular, at higher ridership levels and larger fleet sizes, SFLs *III* and *IV* show increasingly significant reductions in empty kilometers compared to SFLs *I* and *II*. These consistent patterns across both the Belvedere and West Atlanta zones highlight the scalability and robustness of the SAV advantage in minimizing unproductive shuttle movement.

#### 4.6 Analysis of Ridesharing Rates

Figure 9 presents the ridesharing rates for Belvedere and West Atlanta for different fleet sizes. The ridesharing rate is defined as the proportion of total kilometers traveled by the fleet while carrying more than one passenger. As expected, ridesharing rates decrease with larger fleet sizes as a greater number of shuttles allows for more flexible routing and reduces the need to pool trips together for the same trips. At lower fleet sizes, ridesharing rates generally increase with higher demand, as a larger pool of trips raises the likelihood of shared trips. At higher fleet sizes, however, ridesharing rates tend to stabilize, as the available fleet can accommodate increased demand without requiring additional pooling.

Between Belvedere and West Atlanta, ridesharing patterns differ, and overall, the impact of SFLs on ridesharing is not evident. In Belvedere, ridesharing rates are consistently higher for SAVs across all ridership and fleet size scenarios. However, in West Atlanta, SAVs exhibit lower ridesharing rates at lower ridership levels but higher rates compared to human-driven shuttles as demand increases. This indicates that ridesharing rates are highly dependent on spatial and temporal factors, which in turn shape how different SFLs affect the extent of shared travel.

Overall, ridesharing levels were relatively low. However, this outcome is expected given the geo-fenced nature of the zones, which cover small areas and consequently result in shorter trips that must be completed within a zone. Furthermore, a separate ODMTS study similarly found that ridesharing among human drivers exhibited moderate ridesharing rates, which is consistent with the findings of this study [Auad et al., 2021]. These insights collectively suggest that a modest fleet size has the potential to serve even more users

effectively.

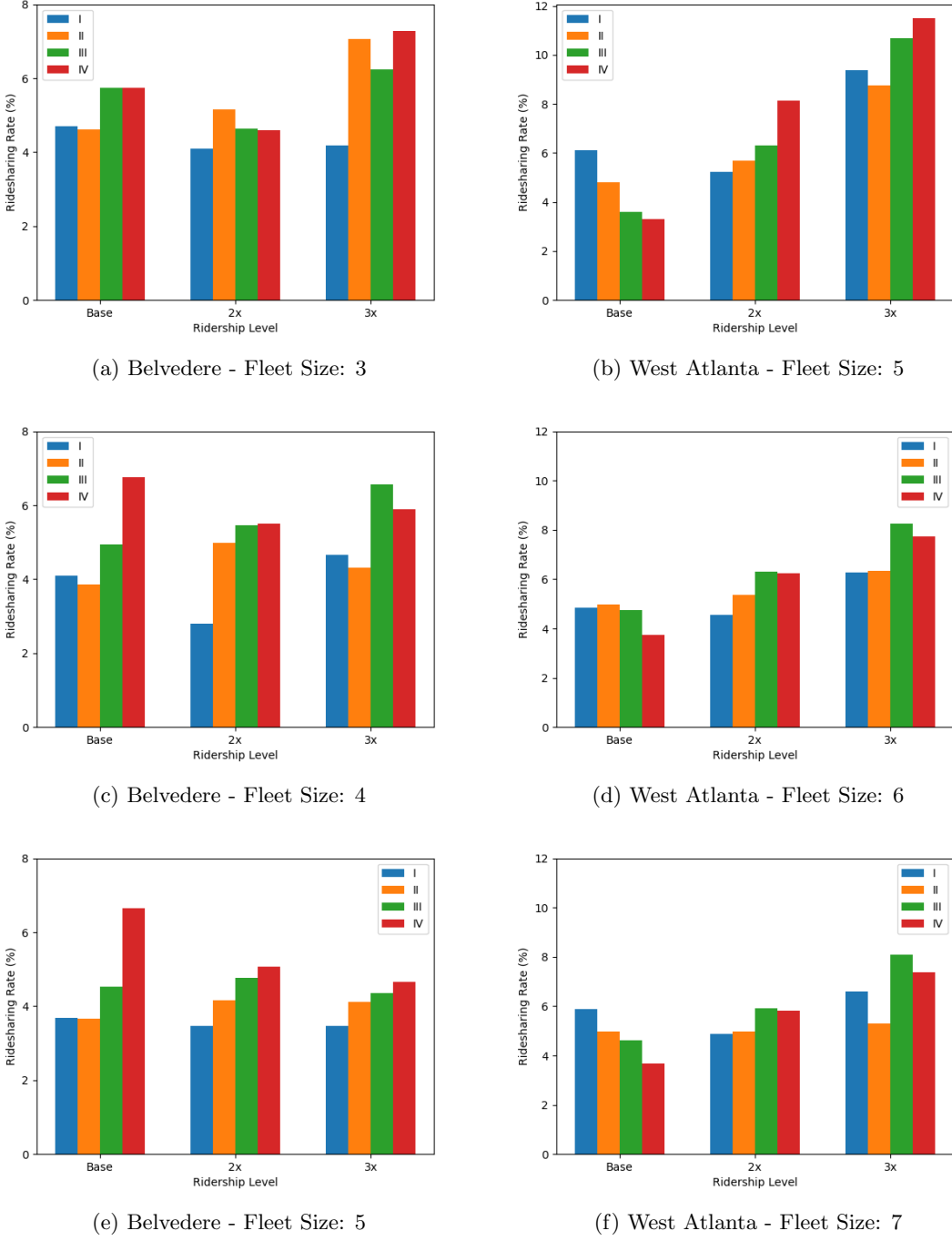


Figure 9: Average Ridesharing Rates

## 4.7 Analysis of Operational Costs

Tables 8 and 9 present the sensitivity analysis of cost per trip across varying operational costs per shuttle per hour for Belvedere and West Atlanta, respectively. Cost per trip was used instead of cost per user because

operational costs are more directly associated with each trip than with the number of users per trip. The cost per shuttle per hour parameters are hypothetical and are used solely for sensitivity analysis. The cost per shuttle per hour was multiplied by the total hours of operation and the number of shuttles, and then divided by the number of trips to obtain the cost per trip per hour of service. Regardless of the SFL, the cost per trip remains consistent because the number of riders served does not change across SFLs. Moreover, labor costs are assumed to remain consistent across SFLs. While SAVs eliminate the need for human drivers, operational labor may still be required to monitor SAVs while in service. Recent developments in SAV-based mobility services have shown that operators often include attendants on board to greet passengers, provide service information, and intervene manually if necessary. In addition, SAV operators increasingly rely on command center agents who remotely monitor vehicles and provide assistance when issues arise outside the operational domain [Beep, 2025].

Evidently, the cost per trip increases with larger fleet sizes, as the higher operational costs outpace the corresponding increase in ridership. However, this higher cost per trip is accompanied by an improvement in service quality from the expanded fleet capacity. The results also indicate that the cost per trip decreases substantially as ridership increases.

For MARTA Reach shuttles with a capacity of eight passengers, the average cost per shuttle per hour is estimated between \$50 to \$70 [Van Hentenryck et al., 2023]. In contrast, ridesharing services such as uber typically use compact vehicles such as sedans, which have a capacity of four passengers and a per-vehicle operating cost of approximately \$26.35 per vehicle hour, including labor and operating expenses [Helling et al., 2023]. Therefore, minivan shuttles with a capacity of six passengers are estimated to have an average operating cost between \$35 and \$50 per hour. This results in a cost per trip between \$31.74 to \$75.58 in Belvedere and \$25.56 and \$51.12 in West Atlanta at base ridership levels. As public transit is highly subsidized, fare revenues cover only a portion of operating expenses. MARTA fares specifically accounted for only 12.2% of the total operating expenses in 2022 [Federal Transit Administration, 2022], with a fixed fare of \$2.50 per trip. To maintain an equivalent fare-to-cost ratio, the subsequent fares would range from \$3.87 to \$9.22 per trip in Belvedere and \$3.11 to \$6.24 in West Atlanta. At higher demand levels, the cost per trip lies between \$11.19 and \$26.64 in Belvedere and \$8.43 and \$16.85 in West Atlanta, with corresponding adjusted fares ranging from \$1.37 to \$3.25 in Belvedere and \$1.03 and \$2.06 in West Atlanta, which are comparable to, and potentially less expensive than, MARTA's current transit fare. This suggests that integrating on-demand minivan shuttles to complement bus service could yield substantial cost savings for public transit agencies, with increasing returns at scale with demand. This is particularly relevant, as the pilot data showed a continuous increase in demand toward its conclusion, indicating the potential for more cost-efficient operations.

Additional scenarios with higher cost per shuttle per hour values are provided in Appendix B.

## 5 Conclusion

This paper investigated the impact of SAVs in microtransit systems, alongside other operational features. To implement this study, a RTDARS modeling framework was employed and enhanced with to incorporate both human-driven and SAV shuttle dispatching and routing. Human-driven shuttles were modeled with delayed driver response times to trip requests while idling and were subject to safety protocols that prohibited re-routing while en route between stops. SAVs enabled dynamic re-routing to accommodate on-demand trip requests while in operation and exhibited zero-delay responses to trip requests. Additionally, a MPC

Shuttle Cost	$ N  = 39$ : 1x (Base)			$ N  = 78$ : 2x			$ N  = 117$ : 3x		
	$ V  = 3$	$ V  = 4$	$ V  = 5$	$ V  = 3$	$ V  = 4$	$ V  = 5$	$ V  = 3$	$ V  = 4$	$ V  = 5$
20	18.14	24.19	30.23	9.51	12.68	15.85	6.39	8.52	10.66
25	22.67	30.23	37.79	11.89	15.85	19.82	7.99	10.66	13.32
30	27.21	36.28	45.35	14.27	19.02	23.78	9.59	12.79	15.98
35	31.74	42.33	52.91	16.65	22.20	27.74	11.19	14.92	18.65
40	36.28	48.37	60.47	19.02	25.37	31.71	12.79	17.05	21.31
45	40.81	54.42	68.02	21.40	28.54	35.67	14.39	19.18	23.98
50	45.35	60.47	75.58	23.78	31.71	39.63	15.98	21.31	26.64

Table 8: Cost (\$) per trip in Belvedere Across Ridership Levels. Shuttle costs are in \$/hour.

Shuttle Cost	$ N  = 82$ : 1x (Base)			$ N  = 164$ : 2x			$ N  = 246$ : 3x		
	$ V  = 5$	$ V  = 6$	$ V  = 7$	$ V  = 5$	$ V  = 6$	$ V  = 7$	$ V  = 5$	$ V  = 6$	$ V  = 7$
20	14.61	17.53	20.45	7.14	8.57	10.00	4.81	5.78	6.74
25	18.26	21.91	25.56	8.93	10.71	12.50	6.02	7.22	8.43
30	21.91	26.29	30.67	10.71	12.86	15.00	7.22	8.67	10.11
35	25.56	30.67	35.79	12.50	15.00	17.50	8.43	10.11	11.80
40	29.21	35.06	40.90	14.29	17.14	20.00	9.63	11.56	13.48
45	32.87	39.44	46.01	16.07	19.29	22.50	10.83	13.00	15.17
50	36.52	43.82	51.12	17.86	21.43	25.00	12.04	14.44	16.85

Table 9: Cost (\$) per trip in West Atlanta Across Ridership Levels. Shuttle costs are in \$/hour.

approach was developed for shuttle rebalancing toward designated idle locations without relying on extensive historical data, where two optimization models were proposed to determine optimal shuttle rebalancing strategies.

Scenario-based experiments were designed on varying SFLs, fleet sizes, and demand levels. A case study was implemented in the metropolitan Atlanta area using operational and ridership data from the MARTA Reach Pilot, the first pilot of ODMTS in Atlanta. The results demonstrated that incorporating SAVs in microtransit system operations can significantly reduce user waiting times without compromising travel times while improving overall system efficiency through reductions in total travel distance and empty kilometers driven. The analysis of ridership and fleet size variations further illustrated how these benefits could scale between supply and demand. The cost analysis revealed that microtransit systems can yield cost savings with increasing demand while improving higher service quality.

Through this design framework, this study provides further justification for the viability of the ODMTS prototype and potential success of microtransit systems as a next-generation transit solution. While the MARTA Reach Pilot effectively connected riders to employment, healthcare, food, and other essential destinations, the integration of the technologies and operational strategies presented here could further enhance system performance.

Future research could examine the impact of electric vehicles and charging infrastructure within microtransit systems, which would introduce additional operational constraints related to shuttle range and charging availability. Additional work could also address the real-world challenges in integration of AVs as extensions to public transit systems. From a methodological perspective, further research may focus on incorporating multimodal transit incentive programs in microtransit systems to enhance user adoption [Lu and Masoud, 2025b]. Further works on microtransit systems could connect other mobility services to integrate

with the system as first- and last-mile connectors such as bikesharing and e-scooters [Lim et al., 2022].

## Acknowledgments

This research was partly supported by NSF CIVIC grant No. 2133342, NSF Leap-HI grant No. 1854684, and NSF grant No. 2046372. The authors would like to thank PhD Student Jorge Huertas at Georgia Tech for providing benchmark visuals for this paper. The authors would like to thank MARTA for a successful collaboration.

## Appendix A Vehicle Rebalancing Optimization with Tie-Breaking

Model (3) may produce ties in the ratio of mapped requests to shuttles at idle stops. However, resolving ties prematurely in this model could lead to poor relocation decisions.

Consider a set of idle stops  $X \subseteq S_{idle}$  that exhibit ratio ties. In an example, suppose idle stops  $s_a \in X$  and  $s_b \in X$  are tied, and that each currently has two vehicles allocated. Suppose also that there are three vehicles located near stop  $s_a$  and no vehicles near stop  $s_b$ . In this example, to minimize total vehicle relocation time, and thereby maximize vehicle availability, the tie-breaking procedure should allocate the majority of vehicles to stop  $s_a$ . This example illustrates two key principles: 1) tie-breaking only matters when  $|X|$  is greater than the remaining idle vehicles left to assign; and 2) that effective tie-breaking requires knowledge of individual vehicle locations. Thus, tie-breaking should occur during the assignment of vehicles for relocation.

Model (5) modifies Model (4) to account for the relocation at tied idle locations. Constraint (5b) is analogous to constraint (4b) for idle locations that do not require tie-breaking. For all stops  $s \in X$ , either  $v_s$  or  $v_s + 1$  vehicles could be assigned, as shown in constraints (5c) and (5d). This flexibility allows more informed tie-breaking while minimizing total travel time.

$$\text{minimize} \quad (4a), \quad (5a)$$

$$\text{subject to} \quad \sum_{v \in \hat{V}_{idle}} w_s^v = v_s \quad \forall s \in S_{idle} \setminus X, \quad (5b)$$

$$\sum_{v \in \hat{V}_{idle}} w_s^v \geq v_s \quad \forall s \in X, \quad (5c)$$

$$\sum_{v \in \hat{V}_{idle}} w_s^v \leq v_s + 1 \quad \forall s \in X, \quad (5d)$$

$$(4c), (4d)$$

## Appendix B Additional Scenarios of Operational Costs

Tables 10 and 11 present additional sensitivity analysis of cost per trip at higher operational costs per shuttle per hour for Belvedere and West Atlanta, respectively.

Shuttle Cost	N  = 39: 1x (Base)			N  = 78: 2x			N  = 117: 3x		
	V  = 3	V  = 4	V  = 5	V  = 3	V  = 4	V  = 5	V  = 3	V  = 4	V  = 5
55	49.88	66.51	83.14	26.16	34.88	43.60	17.58	23.44	29.30
60	54.42	72.56	90.70	28.54	38.05	47.56	19.18	25.57	31.97
65	58.95	78.60	98.26	30.91	41.22	51.52	20.78	27.70	34.63
70	63.49	84.65	105.81	33.29	44.39	55.49	22.38	29.84	37.30
75	68.02	90.70	113.37	35.67	47.56	59.45	23.98	31.97	39.96
80	72.56	96.74	120.93	38.05	50.73	63.41	25.57	34.10	42.62
85	77.09	102.79	128.49	40.43	53.90	67.38	27.17	36.23	45.29
90	81.63	108.84	136.05	45.18	60.24	75.30	28.77	38.36	47.95
95	86.16	114.88	143.60	47.56	63.41	79.27	30.37	40.49	50.61
100	90.70	120.93	151.16	50.00	66.67	83.33	31.97	42.62	53.28

Table 10: Cost (\$) per trip in Belvedere Across Ridership Levels. Shuttle costs are in \$/hour.

Shuttle Cost	N  = 82: 1x (Base)			N  = 164: 2x			N  = 246: 3x		
	V  = 5	V  = 6	V  = 7	V  = 5	V  = 6	V  = 7	V  = 5	V  = 6	V  = 7
55	40.17	48.20	56.24	19.64	23.57	27.50	13.24	15.89	18.54
60	43.82	52.58	61.35	21.43	25.71	30.00	14.44	17.33	20.22
65	47.47	56.97	66.46	23.21	27.86	32.50	15.65	18.78	21.91
70	51.12	61.35	71.57	25.00	30.00	35.00	16.85	20.22	23.59
75	54.78	65.73	76.69	26.79	32.14	37.50	18.06	21.67	25.28
80	58.43	70.11	81.80	28.57	34.29	40.00	19.26	23.11	26.96
85	62.08	74.49	86.91	30.36	36.43	42.50	20.46	24.56	28.65
90	65.73	78.88	92.02	32.14	38.57	45.00	21.67	26.00	30.33
95	69.38	83.26	97.13	33.93	40.71	47.50	22.87	27.44	32.02
100	73.03	87.64	102.25	35.71	42.86	50.00	24.07	28.89	33.70

Table 11: Cost (\$) per trip in West Atlanta Across Ridership Levels. Shuttle costs are in \$/hour.

## References

A. Aalipour and A. Khani. Modeling, analysis, and control of autonomous mobility-on-demand systems: a discrete-time linear dynamical system and a model predictive control approach. *IEEE Transactions on Intelligent Transportation Systems*, 25(8):8615–8628, 2024.

J. Alonso-Mora, S. Samaranayake, A. Wallar, E. Frazzoli, and D. Rus. On-demand high-capacity ride-sharing via dynamic trip-vehicle assignment. *Proceedings of the National Academy of Sciences*, 114(3):462–467, 2017. doi: 10.1073/pnas.1611675114.

R. Auad, K. Dalmeijer, C. Riley, T. Santanam, A. Trasatti, P. Van Hentenryck, and H. Zhang. Resiliency of on-demand multimodal transit systems during a pandemic. *Transportation Research Part C: Emerging Technologies*, 133:103418, 2021.

B. Basciftci and P. Van Hentenryck. Capturing travel mode adoption in designing on-demand multimodal transit systems. *Transportation Science*, 57(2):351–375, 2023.

Beep. <https://ridebeep.com/solutions/operations>, 2025.

C. V. Beojone and N. Geroliminis. On the inefficiency of ride-sourcing services towards urban congestion. *Transportation research part C: emerging technologies*, 124:102890, 2021.

M. Bruglieri, R. Peruzzini, and O. Pisacane. Efficiently routing a fleet of autonomous vehicles in a real-time ride-sharing system. *Computers & Operations Research*, 168:106668, 2024.

J. Bürstein, D. López, and B. Farooq. Exploring first-mile on-demand transit solutions for north american suburbia: A case study of markham, canada. *Transportation Research Part A: Policy and Practice*, 153: 261–283, 2021.

J. F. Campbell, A. T. Ernst, and M. Krishnamoorthy. Hub arc location problems: part i—introduction and results. *Management Science*, 51(10):1540–1555, 2005.

N. D. Chan and S. A. Shaheen. Ridesharing in north america: Past, present, and future. *Transport reviews*, 32(1):93–112, 2012.

Chatham Area Transit. <https://catchacat.org/smart/>, 2025.

J.-F. Cordeau and G. Laporte. The dial-a-ride problem: Models and algorithms. *Annals of Operations Research*, 153(1):29–46, 2007. doi: 10.1007/s10479-007-0170-8.

G. D. Erhardt, S. Roy, D. Cooper, B. Sana, M. Chen, and J. Castiglione. Do transportation network companies decrease or increase congestion? *Science advances*, 5(5):eaau2670, 2019.

Federal Transit Administration. National Transit Database, 2022. URL <https://www.transit.dot.gov/ntd>.

R. Griffin, C. Huisingsh, and G. McGwin Jr. Prevalence of and factors associated with distraction among public transit bus drivers. *Traffic injury prevention*, 15(7):720–725, 2014.

H. Guan, B. Basciftci, and P. Van Hentenryck. Bilevel optimization and heuristic algorithms for integrating latent demand into the design of large-scale transit systems. *arXiv preprint arXiv:2212.03460*, 2025.

A. Hart. Marta: “stringent” ban on driver distractions, Dec 2009. URL <https://www.ajc.com/news/local/marta-stringent-ban-driver-distractions/tWi4NBV6FoioHixvRITJeK/#:~:text=Under%20the%20ban%2C%20employees%20may,otherwise%20engaging%20in%20distracting%20activities>.

B. Helling, Stephen, E. Hempler, Paul, Q. Williams, S. Savage, and Tom. The real costs of driving for uber and lyft [2023 update]. <https://www.ridester.com/uber-lyft-driver-costs-and-expenses/>, Jan 2023.

A. Henao and W. E. Marshall. The impact of ride-hailing on vehicle miles traveled. *Transportation*, 46(6): 2173–2194, 2019.

M. Kodransky and G. Lewenstein. *Connecting low-income people to opportunity with shared mobility*. ITDP, 2014.

A. Y. Lam, Y.-W. Leung, and X. Chu. Autonomous-vehicle public transportation system: Scheduling and admission control. *IEEE Transactions on Intelligent Transportation Systems*, 17(5):1210–1226, 2016.

J. Lazarus, S. Shaheen, S. E. Young, D. Fagnant, T. Voege, W. Baumgardner, J. Fishelson, and J. Sam Lott. *Shared automated mobility and public transport*. Springer, 2018.

M. W. Levin, M. Odell, S. Samarasena, and A. Schwartz. A linear program for optimal integration of shared autonomous vehicles with public transit. *Transportation Research Part C: Emerging Technologies*, 109: 267–288, 2019.

J. Lim, K. Dalmeijer, S. Guhathakurta, and P. Van Hentenryck. The bicycle network improvement problem. *Journal of Transportation Engineering, Part A: Systems*, 148(11):04022095, 2022.

T. Litman. Autonomous vehicle implementation predictions: Implications for transport planning. 2020.

M. Lowalekar, P. Varakantham, and P. Jaillet. Zac: A zone path construction approach for effective real-time ridesharing. In *Proceedings of the 2018 Conference on Automated Planning and Scheduling*, 2018.

J. Lu and N. Masoud. The incentive bundle program to enhance multimodal transportation. *Preprint on ResearchGate*, 2025a.

J. Lu and N. Masoud. Incentive design for mobility services: A review and future directions. *Preprint on ResearchGate*, 2025b.

J. Lu, A. Trasatti, H. Guan, K. Dalmeijer, and P. Van Hentenryck. The impact of congestion and dedicated lanes on on-demand multimodal transit systems. *Travel Behaviour and Society*, 36:100772, 2024. doi: 10.1016/j.tbs.2024.100772.

A. Maheo, P. Kilby, and P. Van Hentenryck. Benders decomposition for the design of a hub and shuttle public transit system. *Transportation Science*, 53(1):77–88, 2019.

K. McCoy, J. Andrew, R. Glynn, W. Lyons, et al. Integrating shared mobility into multimodal transportation planning: Improving regional performance to meet public goals. Technical report, United States. Federal Highway Administration. Office of Planning., 2018.

Mercedes. Eqv. an all-electric 7-seater vehicle. <https://www.mercedes-benz.co.uk/passengercars/models/van/eqv/overview.html>, 2025.

M. T. Ng, H. S. Mahmassani, Ö. Verbas, T. Cokyasar, and R. Engelhardt. Redesigning large-scale multimodal transit networks with shared autonomous mobility services. *Transportation Research Part C: Emerging Technologies*, 168:104575, 2024.

OpenStreetMap contributors. Planet dump retrieved from <https://planet.osm.org>. <https://www.openstreetmap.org>, 2017.

H. K. Pinto, M. F. Hyland, H. S. Mahmassani, and I. Ö. Verbas. Joint design of multimodal transit networks and shared autonomous mobility fleets. *Transportation Research Part C: Emerging Technologies*, 113:2–20, 2020.

C. Riley, A. Legrain, and P. Van Hentenryck. Column generation for real-time ride-sharing operations. In *Integration of Constraint Programming, Artificial Intelligence, and Operations Research: 16th International Conference, CPAIOR 2019, Thessaloniki, Greece, June 4–7, 2019, Proceedings 16*, pages 472–487. Springer, 2019.

C. Riley, P. Van Hentenryck, and E. Yuan. Real-time dispatching of large-scale ride-sharing systems: Integrating optimization, machine learning, and model predictive control. In C. Bessiere, editor, *Proceedings of the Twenty-Ninth International Joint Conference on Artificial Intelligence, IJCAI-20*, pages 4417–4423. International Joint Conferences on Artificial Intelligence Organization, 7 2020. doi: 10.24963/ijcai.2020/609. URL <https://doi.org/10.24963/ijcai.2020/609>. Special track on AI for CompSust and Human well-being.

M. Salazar, F. Rossi, M. Schiffer, C. H. Onder, and M. Pavone. On the interaction between autonomous mobility-on-demand and public transportation systems. In *2018 21st international conference on intelligent transportation systems (ITSC)*, pages 2262–2269. IEEE, 2018.

I. Sanaullah, N. Alsaleh, S. Djavadian, and B. Farooq. Spatio-temporal analysis of on-demand transit: A case study of belleville, canada. *Transportation Research Part A: Policy and Practice*, 145:284–301, 2021.

S. Shaheen and N. Chan. Mobility and the sharing economy: Potential to facilitate the first-and last-mile public transit connections. *Built Environment*, 42(4):573–588, 2016.

Y. Shen, H. Zhang, and J. Zhao. Embedding autonomous vehicle sharing in public transit system: An example of last-mile problem. Technical report, 2017.

Y. Shen, H. Zhang, and J. Zhao. Integrating shared autonomous vehicle in public transportation system: A supply-side simulation of the first-mile service in singapore. *Transportation Research Part A: Policy and Practice*, 113:125–136, 2018.

Socially Aware Mobility Lab. How On-Demand Multimodal Transit Works. <https://sam.isye.gatech.edu/videos>, 2020.

E. Sogbe, S. Susilawati, and T. C. Pin. First-mile and last-mile externalities: Perspectives from a developing country. *Journal of Transport Geography*, 121:104037, 2024.

C. Standing, S. Standing, and S. Biermann. The implications of the sharing economy for transport. *Transport Reviews*, 39(2):226–242, 2019.

M. Stiglic, N. Agatz, M. Savelsbergh, and M. Gradisar. Enhancing urban mobility: Integrating ride-sharing and public transit. *Computers & Operations Research*, 90:12–21, 2018.

A. Tafreshian, M. Abdolmaleki, N. Masoud, and H. Wang. Proactive shuttle dispatching in large-scale dynamic dial-a-ride systems. *Transportation Research Part B: Methodological*, 150:227–259, 2021. doi: 10.1016/j.trb.2021.06.002.

M. Tsao, R. Iglesias, and M. Pavone. Stochastic model predictive control for autonomous mobility on demand. In *2018 21st International conference on intelligent transportation systems (ITSC)*, pages 3941–3948. IEEE, 2018.

P. Van Hentenryck. On-demand mobility systems can ease commuters' burdens–socially aware transit solutions focus on solving 'first/last mile'challenge. *ISE Mag*, 51(10):28–33, 2019.

P. Van Hentenryck, C. Riley, A. Trasatti, H. Guan, T. Santanam, J. A. Huertas, K. Dalmeijer, K. Watkins, J. Drake, and S. Baskin. Marta reach: Piloting an on-demand multimodal transit system in atlanta. *arXiv preprint arXiv:2308.02681*, 2023.

C. J. Venter. Measuring the quality of the first/last mile connection to public transport. *Research in Transportation Economics*, 83:100949, 2020.

Volkswagen. The 2025 id. buzz electric bus. <https://www.vw.com/en/models/id-buzz.html>, 2025.

B. Wang, S. A. O. Medina, and P. Fourie. Simulation of autonomous transit on demand for fleet size and deployment strategy optimization. *Procedia computer science*, 130:797–802, 2018.

H. Wang and H. Yang. Ridesourcing systems: A framework and review. *Transportation Research Part B: Methodological*, 129:122–155, 2019.

H. Wei, Z. Yang, X. Liu, Z. Qin, X. Tang, and L. Ying. A reinforcement learning and prediction-based lookahead policy for vehicle repositioning in online ride-hailing systems. *IEEE Transactions on Intelligent Transportation Systems*, 25(2):1846–1856, 2023.

X. Wu and D. MacKenzie. Assessing the vmt effect of ridesourcing services in the us. *Transportation Research Part D: Transport and Environment*, 94:102816, 2021.

J. Zgraggen, M. Tsao, M. Salazar, M. Schiffer, and M. Pavone. A model predictive control scheme for intermodal autonomous mobility-on-demand. In *2019 IEEE Intelligent Transportation Systems Conference (ITSC)*, pages 1953–1960. IEEE, 2019.

R. Zhang, F. Rossi, and M. Pavone. Model predictive control of autonomous mobility-on-demand systems. In *2016 IEEE international conference on robotics and automation (ICRA)*, pages 1382–1389. IEEE, 2016.